NRL Report 8329

Design Manual for a Constant Beamwidth Transducer

A. L. Van Buren

Measurements Branch
Underwater Sound Reference Detachment
P.O. Box 8337
Orlando, Florida 32856

October 11, 1979

NAVAL RESEARCH LABORATORY
Washington, D.C.

SECURITY CLASSIFICATION OF THIS PAGE (When Data Entered)

REPORT DOCUMENTATION PAGE

READ INSTRUCTIONS BEFORE COMPLETING FORM

1 REPORT NUMBER: NRL Report 8329	2 GOVT ACCESSION NO. / 3 RECIPIENT'S CATALOG NUMBER
4 TITLE (and Subtitle): DESIGN MANUAL FOR A CONSTANT BEAMWIDTH TRANSDUCER	5 TYPE OF REPORT & PERIOD COVERED: Interim report on a continuing NRL problem
	6 PERFORMING ORG. REPORT NUMBER
7 AUTHOR(s): A. L. Van Buren	8 CONTRACT OR GRANT NUMBER(s)
9 PERFORMING ORGANIZATION NAME AND ADDRESS: Underwater Sound Reference Detachment, Naval Research Laboratory, P.O. Box 8337, Orlando, FL 32856	10 PROGRAM ELEMENT, PROJECT, TASK AREA & WORK UNIT NUMBERS: NRL Problem S02-50, Program Element 61153N-11, Project RR011-08-42
11 CONTROLLING OFFICE NAME AND ADDRESS: Department of the Navy, Office of Naval Research, Arlington, VA 22217	12 REPORT DATE: October 11, 1979
	13 NUMBER OF PAGES: 33
14 MONITORING AGENCY NAME & ADDRESS (if different from Controlling Office)	15 SECURITY CLASS. (of this report): UNCLASSIFIED
	15a DECLASSIFICATION/DOWNGRADING SCHEDULE

16 DISTRIBUTION STATEMENT (of this Report)

Approved for public release; distribution unlimited

17 DISTRIBUTION STATEMENT (of the abstract entered in Block 20, if different from Report)

DDC RECEIVED NOV 20 1979 B

18 SUPPLEMENTARY NOTES

19 KEY WORDS (Continue on reverse side if necessary and identify by block number)

Acoustic radiation	Sonar
Transducers	Directional transducers
Constant beamwidth	Sound receivers
Beam patterns	Sound sources

20 ABSTRACT (Continue on reverse side if necessary and identify by block number)

The theory of a broadband constant beamwidth transducer (CBT) which is based on Legendre function amplitude shading of a spherical cap was described in a previous report, *J. Acoust. Soc. Am.* 64:38-43 (1978). Theoretical calculations showed the CBT to have uniform acoustic loading, extremely low side lobes, virtually no nearfield, an essentially constant beam pattern for all frequencies above a certain cutoff frequency, and a flat transmitting current response over a broad band for piezoelectric drive. In this report formulas suitable for the design of a CBT which is to be used as a

(Continued)

DD FORM 1 JAN 73 1473 EDITION OF 1 NOV 65 IS OBSOLETE S/N 0102-014-6601

SECURITY CLASSIFICATION OF THIS PAGE (When Data Entered)

20. Abstract (Continued)

transmitter and/or receiver are developed. The formulas involve simple algebraic and trigonometric expressions and can be readily evaluated using a pocket calculator. Formulas are developed for the required velocity distribution, limiting beam patterns, directivity index, equivalent two-way beam widths for volume and surface reverberation, shading coefficients for a stepwise implementation of the velocity distribution, size, ceramic mass, bandwidth, source level, transmitting voltage and current responses, and receiving voltage sensitivity. The report concludes with an example illustrating the procedure used to design a CBT with a specified 3 dB half-angle beam pattern, source level, and receiving voltage sensitivity.

CONTENTS

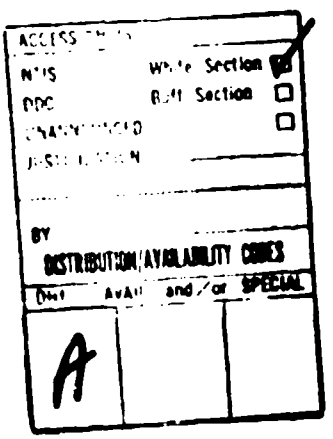

DESIGN MANUAL FOR A CONSTANT BEAMWIDTH TRANSDUCER

INTRODUCTION

Most directional acoustic transducers and arrays exhibit beam patterns which are frequency dependent. Thus, the spectral content of the transmitted or received signal varies with position in the beam and the fidelity of an underwater acoustic system depends on the relative orientation of the transmitter and receiver. In a previous paper [1] we described a simple method for obtaining a transducer whose beamwidth is essentially independent of frequency over a broad bandwidth. Our constant beamwidth transducer (CBT) is a rigid spherical cap of arbitrary half angle α shaded so that the normal velocity on the outer surface is proportional to $P_\nu(\cos\theta)$, where P_ν is the Legendre function whose root of smallest angle occurs at $\theta = \alpha$. The required value for ν, the order of the Legendre function, is not, in general, an integer.

Theoretical calculations show that the CBT has uniform acoustic loading, extremely low sidelobes, and an essentially constant beam pattern for all frequencies above a certain cutoff frequency. Under piezoelectric drive the transducer has a flat transmitting current response over a broad band. In addition, the CBT has virtually no nearfield. The surface pressure distribution as well as the pressure distribution out to the farfield is approximately equal to the surface velocity distribution.

Although the previous report [1] emphasized the transmitter aspects of the CBT, the concept is equally applicable to receivers. The concept is also applicable to an acoustically transparent spherical cap. In fact, Trott [2] has applied the results presented in an earlier unpublished version of [1] to the theoretical design of a receiver CBT using $P_1(\cos\theta) = \cos\theta$ shading on an acoustically transparent hemispherical cap. However, the beam pattern from such a CBT is bidirectional, containing a back lobe identical to the front lobe. For this reason, we will not consider the acoustically transparent case here.

In this report we develop formulas suitable for the design of a CBT which is to be used as a transmitter and/or receiver. The transducer consists of a mosaic of pieces of piezoelectric ceramic bonded to a layer of corprene or other pressure release material which is, in turn, bonded to a backing plate. The formulas involve simple algebraic and trigonometric expressions which can be readily evaluated using a pocket calculator. They are based on excellent approximations for the Legendre functions of noninteger order, and thus avoid the need for evaluating these rarely encountered functions. We obtain formulas for the required velocity distribution, limiting beam pattern, directivity index, equivalent two-way beam widths for volume and surface reverberation, shading coefficients for a stepwise implementation of the velocity distribution, spherical cap size, ceramic mass, bandwidth, source level, transmitting voltage and current response, and receiving voltage sensitivity.

Manuscript submitted May 18, 1979.

The designer of a CBT first chooses the desired beam pattern, characterized by either the - 3 dB half angle or by the cap half angle, which is also the theoretical pattern null. He then specifies the desired source level and/or receiving voltage sensitivity and uses the formulas in this report to calculate the required CBT design together with its predicted acoustic properties. As an example of this procedure, we conclude the report with the design of a CBT that has a - 3 dB half angle of 7°, a source level of 200 dB re 1μ Pa at 1 m, and a receiving voltage sensitivity of - 200 dB re 1 V/μ Pa.

VELOCITY DISTRIBUTION

The key to the special properties of the CBT is its surface normal velocity distribution $v(\theta)$ given by

$$\begin{aligned} v(\theta) &= P_\nu(\cos\theta),\ 0 \le \theta \le \alpha_\nu, \\ v(\theta) &= 0,\ \theta \ge \alpha_\nu, \end{aligned} \tag{1}$$

where α_ν is the zero of smallest angle of the Legendre function $P_\nu(\cos\theta)$. We showed in Ref. 1 that the CBT need not extend beyond α_ν, and thus can be constructed as a spherical cap whose half angle is equal to α_ν. Consequently, we call α_ν the cap-half-angle, although in practice the actual cap-half-angle for a P_ν CBT can possess any value $\theta \ge \alpha_\nu$. The order ν of the Legendre function can be chosen to be any real number greater than zero. The corresponding angle α_ν decreases monotonically from near 180° as ν increases from just above zero. However, in order to obtain the reasonably simple design formulas presented in this report, we restrict ν to be equal to or greater than unity. This simultaneously restricts α_ν to be equal to or less than 90°. We do not expect this restriction to be of any consequence since there do not appear to be many (if any) sonar applications calling for a CBT with α_ν greater than 90°. If such applications do occur, then design formulas corresponding to, but more complicated than, those given in this paper can be obtained for $\nu < 1$. The following approximation for α_ν, in degrees,

$$\alpha_\nu \simeq \frac{137.796}{(\nu+0.5)}\left[1 - \frac{0.045}{(\nu+0.5)^2}\right], \tag{2}$$

is correct to within 0.03% for $\nu \ge 1$. We present in Fig. 1 a graph of α_ν as a function of ν. We also include a graph of the - 3 dB half angle γ_ν, i.e., the value for θ such that $P_\nu^2(\cos\theta) = 0.5$. The following approximation for γ_ν, in degrees,

$$\gamma_\nu \simeq \frac{64.640}{(\nu+0.5)}\left[1 + \frac{0.103}{(\nu+0.5)^2}\right], \tag{3}$$

is believed to be correct to within 0.1% for $\nu \ge 1$.

The Legendre function $P_\nu(\cos\theta)$ is a monotonically decreasing function of θ in the range $0 \le \theta \le \alpha_\nu$. In Fig. 2 we show $P_\nu(\cos\theta)$ over this range for ν = 5, 7.5, and 10.0. The function $P_\nu(\cos\theta)$ can be evaluated to any desired accuracy by use of its hypergeometric expansion in $(1 - \cos\theta)/2$. Fortunately, use of this expansion is unnecessary for our purposes. Sufficiently accurate values over the range $0 \le \theta \le \alpha_\nu$ can be obtained using the

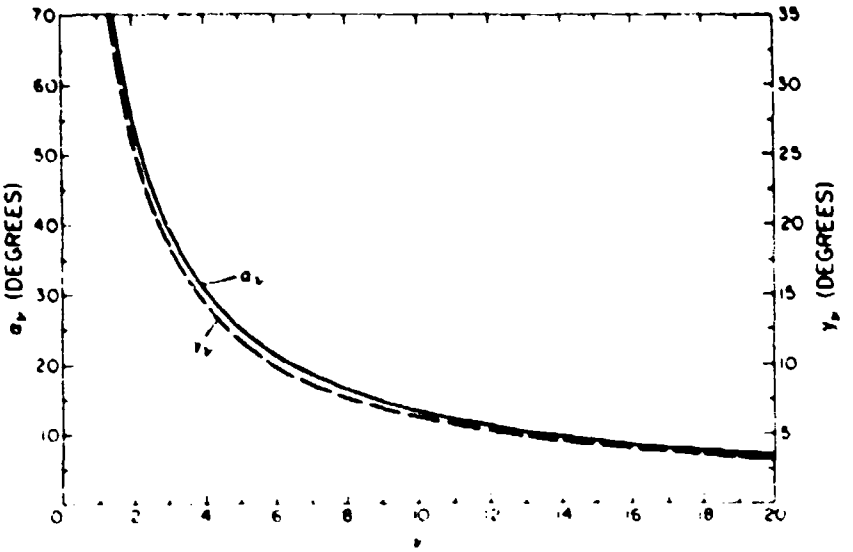

Fig. 1 – Variation of the cap half angle α_ν and the −3 dB half angle γ_ν as a function of the Legendre function order ν

following excellent approximation in terms of the zeroth order cylindrical Bessel function of the first kind:

$$P_\nu(\cos\theta) \simeq [\pi\theta/(180\sin\theta)]^{1/2} J_0(2.40480\theta/\alpha_\nu), \tag{4}$$

with both θ and α_ν given in degrees. For $\nu = 1$, the error in Eq. (4) is less than 0.1% for $0 \leq \theta \leq 35°$, less than 0.2% for $35° \leq \theta \leq 55°$, and less than 0.4% over the remainder of the range $55° \leq \theta \leq 90°$. The error decreases rapidly with increasing ν.

For large values of ν, the range of θ is small and the factor $[\pi\theta/(180\sin\theta)]^{1/2}$ approaches unity and can be discarded. Thus for large ν, we obtain the simpler approximation

$$P_\nu(\cos\theta) \simeq J_0(2.40480\theta/\alpha_\nu). \tag{5}$$

Graphs of $P_\nu(\cos\theta)$ and $J_0(2.40480\theta/\alpha_\nu)$ as a function of θ/α_ν are shown in Fig. 3 for $\nu = 1$ and 2. The agreement between $J_0(2.40480\theta/\alpha_\nu)$ and $P_\nu(\cos\theta)$ for $0 \leq \theta \leq \alpha_\nu$ improves rapidly with increasing ν, being reasonably good at $\nu = 1$ and very good for $\nu = 2$. Graphs of the closer approximation given by Eq. (4) for $\nu = 1$ and 2 would be indistinguishable from the curves shown in Fig. 3 for $P_1(\cos\theta)$ and $P_2(\cos\theta)$, respectively. Accurate numerical values for the Bessel function $J_0(x)$ can either be calculated using the polynomial approximations given in Abramowitz and Stegun [3] or obtained from tables such as those given in Refs. 4 and 5.

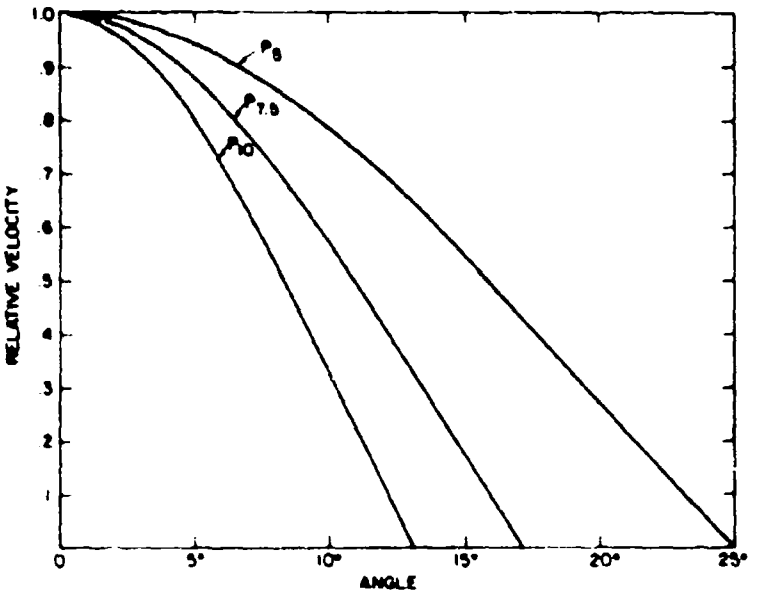

Fig. 2 – Velocity shading functions for a P_8 CBT, a $P_{7.8}$ CBT, and a P_{10} CBT

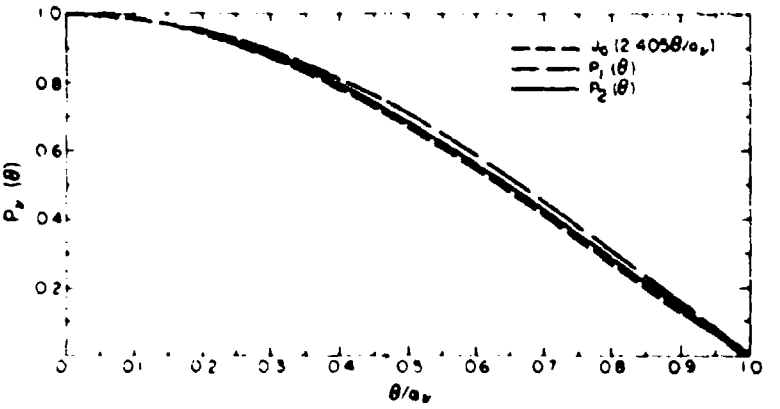

Fig. 3 – Comparison of $P_\nu(\cos\theta)$ and $J_0(2.405\theta/\alpha_\nu)$ as a function of θ/α_ν for $\nu = 1$ and 2

We obtain from Eq. (4) with $\nu = 1$:

$$P_1(\cos\theta) = \cos\theta \simeq [\pi\theta/(180 \sin\theta)]^{1/2} J_0(2.4048\,\theta/90), \tag{6}$$

for $0 \leq \theta \leq \alpha_1 = 90°$. We can invert this equation to provide the following approximation for $J_0(x)$:

$$J_0(x) \simeq \left[\frac{\sin(90x/2.4048}{\pi x/4.8096}\right]^{1/2} \cos(90x/2.4048), \tag{7}$$

where the arguments of both sin and cos are in degrees. The relative error in this approximation increases monotonically from 0% to a maximum of almost 0.4% as x increases from zero to just below the first root of $J_0(x)$ at $x = 2.4048$. As x increases from just above the first root to a value near π, the relative error decreases monotonically from nearly 0.4% to less than 0.01%. Beyond $x = \pi$, the relative error increases rapidly, being 0.4% at $x = 3.35$ and 4.7% at $x = 4.0$.

We can substitute J_0 from Eq. (7) into Eq. (4) to obtain the following approximation for $P_\nu(\cos\theta)$, $0 \leq \theta \leq \alpha_\nu$, in terms of trigonometric functions:

$$P_\nu(\cos\theta) \simeq \left[\frac{\sin(90\,\theta/\alpha_\nu)}{(90/\alpha_\nu)\sin\theta}\right]^{1/2} \cos(90\,\theta/\alpha_\nu), \tag{8}$$

where again the arguments of sin and cos are in degrees. Because of the nature of its derivation, this approximation is exact for $\nu = 1$. For $\nu > 1$ and $0 < \theta < \alpha_\nu$, the approximation is always somewhat larger than $P_\nu(\cos\theta)$. The relative error for all $\nu > 1$ increases as θ approaches α_ν and reaches a maximum of less than 0.4% for values of θ just less than α_ν. We believe that the approximation given in Eq. (8) is quite adequate for most purposes in designing a CBT.

BEAM PATTERNS

The beam pattern $g(\theta)$ of a P_ν CBT approaches the normal velocity distribution in the limit of high frequency. Thus, the limiting pattern is rotationally symmetrical, has a maximum in the direction of the axis of the spherical cap, decreases monotonically to zero at the cap half angle α_ν, and is equal to zero for $\theta \geq \alpha_\nu$. Approximations for both the pattern null α_ν and the -3 dB half angle γ_ν in terms of ν were given as Eqs. (2) and (3), respectively, in the second section. Approximations for the velocity distribution given by Eqs. (4), (5), and (8) in the Introduction are also appropriate for describing the limiting beam patterns.

As the frequency decreases from high to low values, the CBT beam patterns tend to resemble the high frequency limit less and less. The highest frequency below which the resemblance is less than acceptable is called the low-frequency cutoff f_c. A general rule of thumb for the cutoff frequency f_c in kHz is given by

$$f_c = c[1.10 + (24.6/\gamma_\nu)]/(1500\,b), \tag{9a}$$

where c is the sound speed of the surrounding fluid in m/sec, b is the half-arclength (i.e., radius) of the spherical cap in meters, and γ_ν is in degrees. By use of Eqs. (2) and (3) we can alternately express f_c in terms of the cap half angle α_ν in degrees by

$$f_c \simeq c[1.10 + (52.5/\alpha_\nu)(1 - 7.79 \times 10^{-6}\alpha_\nu^2)]/(1500\, b), \tag{9b}$$

or, in terms of the Legendre function order ν by

$$f_c \simeq c[1.10 + 0.381\,(\nu + 0.5)\{1 - 0.103/(\nu + 0.5)^2\}]/(1500\, b). \tag{9c}$$

If a is the radius of curvature of the cap, then $b = \pi a\alpha_\nu/180$.

Since Eqs. (9a) to (9c) are only general rules of thumb, we use a value of 1500 m/sec for the sound speed c when calculating f_c for a CBT to be used in water, even though the actual sound speed of the water might be somewhat different than this. The cutoff frequency f_c and the inverse of the cap radius scale together. We define as the frequency constant for a CBT radiating into water the quantity $F_\nu = f_c b = 1.10 + (24.6/\gamma_\nu)$. A graph of the behavior of the frequency constant F_ν as a function of the -3 dB half-angle γ_ν is shown in Fig. 4. We note that the definition for f_c given above differs slightly for low ν from that given in Ref. 1. The difference is only 1.4% at $\nu = 1$ and decreases rapidly with increasing ν.

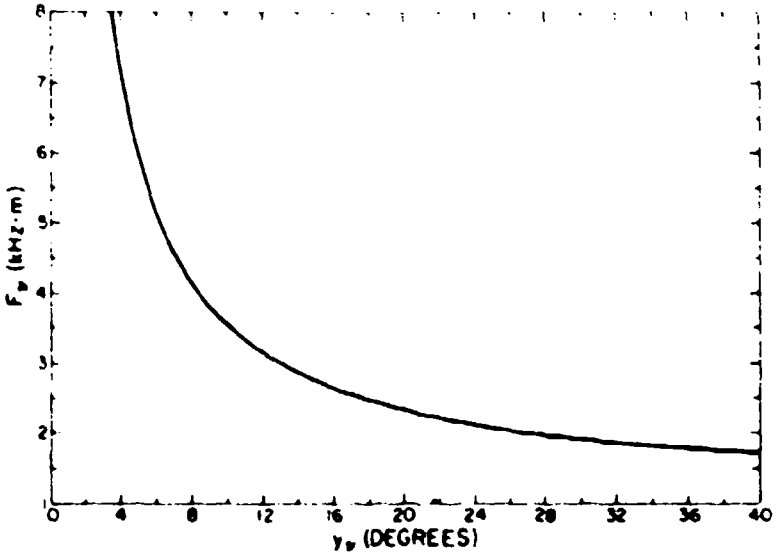

Fig. 4 — Frequency constant F_ν in kHz·m as a function of the -3 dB half angle γ_ν in degrees

The choice of the frequency below which the beam patterns are unacceptable is a subjective one and depends strongly on the applications that the user has in mind for the CBT. As an example, we show in Fig. 5 calculated beam patterns for a $P_{2.75}$ CBT. The -3 dB half angle for $P_{2.75}$ is 20°. The beam pattern at 10 f_c is indistinguishable from the $P_{2.75}$ velocity distribution. The beam pattern at 3 f_c for angles less than about 32° is nearly identical with that at 10 f_c, however, the two patterns differ somewhat for larger angles. The same is true for 2 f_c, although the deviation from the 10 f_c beam pattern for $\theta > 32°$ is more substantial. As the frequency is decreased below 2 f_c, we begin to see a significant deviation from the 10 f_c beam pattern for $\theta > 32°$. The deviation for angles above 32° appears to increase monotonically with decreasing frequency, however, the deviation below 32° is greater at 1.2 f_c than at f_c or 0.8 f_c. Examination of the extrema curves presented in Ref. 1 for P_5, $P_{7.5}$, and P_{10} CBT's suggests that the portion of the beam pattern around the -10 dB angle changes less with frequency than any other part of the pattern. Thus, if we are primarily concerned with the constancy of the beam pattern for angles less than the -10 dB angle, and only require that there be no substantial sidelobes for higher angles, then the cutoff frequency for $P_{2.75}$ can be chosen as low as 0.8 f_c. On the other hand, if constancy of the beam pattern for larger angles is required, then the cutoff frequency must be chosen somewhat larger than f_c.

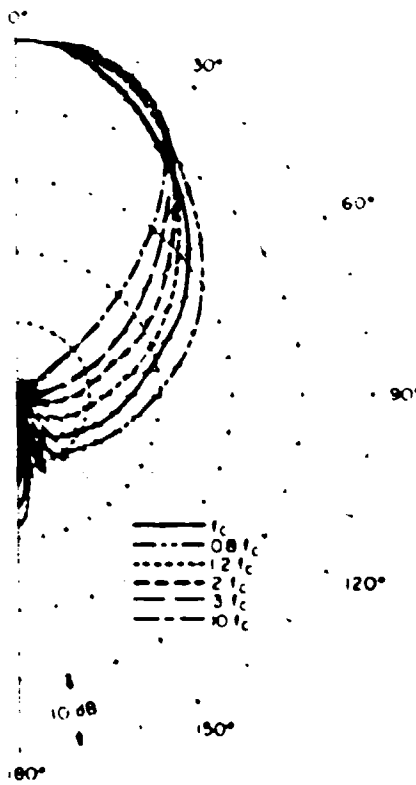

Fig. 5 — Calculated beam patterns for a $P_{2.75}$ CBT at selected relative frequencies f/f_c

For additional information on the variation of the CBT beam patterns with frequency, we reproduce here the extrema curves given in Ref. 1. Figures 6, 7, and 8 show the calculated range of beam patterns for a P_5 CBT, a $P_{7.5}$ CBT, and P_{10} CBT, respectively, both for frequencies above the cutoff frequency f_c (indicated by the total shaded region) and for frequencies above $2f_c$ (indicated by the dark shaded region).

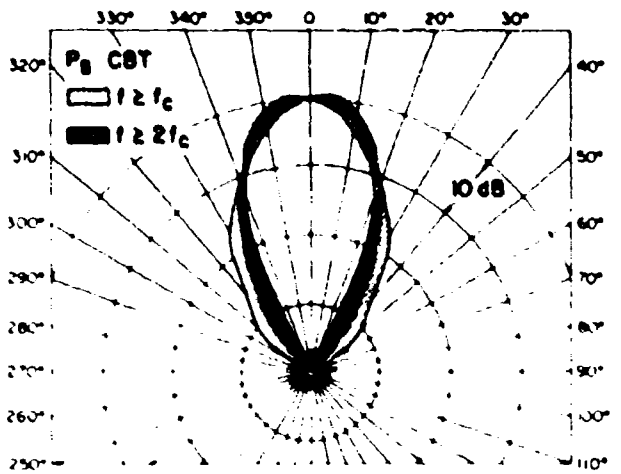

Fig. 6 — Range of Beam patterns for P_5 CBT for $f \geq f_c$ (total shaded area) and $f \geq 2f_c$ (dark shaded area only)

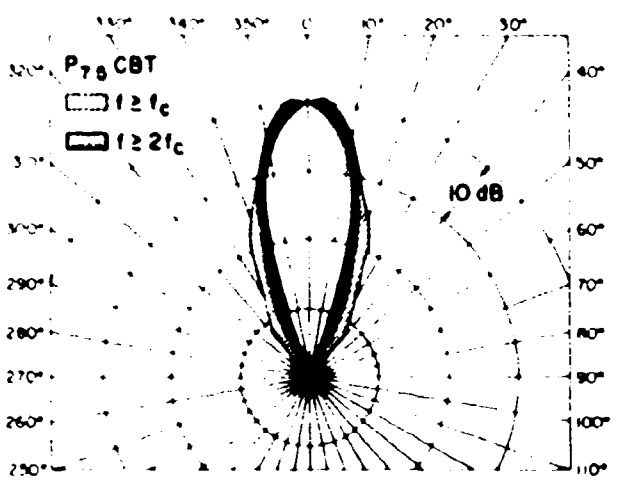

Fig. 7 — Range of beam patterns for $P_{7.5}$ CBT for $f \geq f_c$ (total shaded area) and $f \geq 2f_c$ (dark shaded area only)

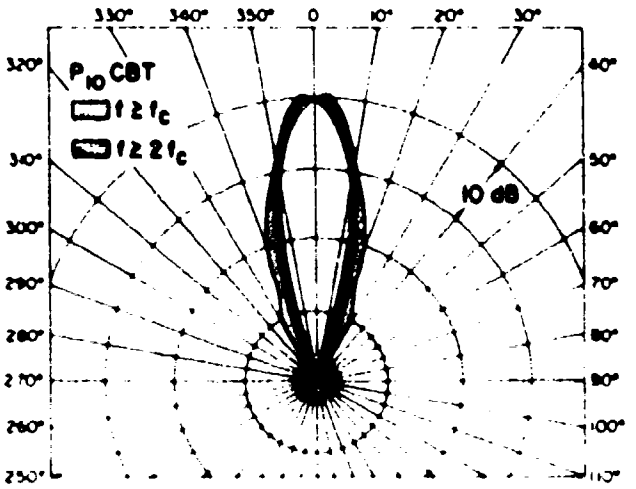

Fig. 8 — Range of beam patterns for P_{10} CBT for $f \geq f_c$ (total shaded area and $f \geq 2\ f_c$ (dark shaded area only)

In the next three sections of this report we will derive (for the limiting beam patterns) excellent approximations for the directivity index and for both the surface and volume reverberation two-way beamwidths of the CBT.

DIRECTIVITY INDEX

The directivity index DI for a CBT is given by

$$DI = -10 \log_{10} \left[\frac{1}{2} \int_0^{\pi \alpha_\nu / 180} P_\nu^{\,2}(\cos\theta) \sin\theta d\theta \right]. \tag{10}$$

Rewriting Eq. (4) so that θ is in radians, substituting the resulting expression for $P_\nu(\cos\theta)$ into Eq. (10), and integrating exactly, we obtain the approximation

$$DI \simeq -10 \log_{10} [0.25\pi^2 \alpha_\nu^{\,2} J_1^{\,2}(2.4048)/(180)^2],$$

or (11a)

$$DI \simeq -20 \log_{10} \alpha_\nu + 46.88,$$

with α_ν in degrees.

We can alternately express the result in terms of ν by use of Eq. (2) to give

$$DI \simeq 20 \log_{10} (\nu + 0.5) + 4.09 + [0.391/(\nu + 0.5)^2]. \tag{11b}$$

Eqs. (3) and (11b) can then be used to obtain the corresponding expression for DI in terms of the - 3 dB half angle y_ν in degrees:

$$DI \simeq -20 \log_{10} y_\nu + 40.29 + 3.09 \times 10^{-4} y_\nu^2. \tag{11c}$$

All three approximations are accurate to within 0.1 dB for $\nu = 1$, and increase rapidly in accuracy with increasing ν. We show in Fig. 9 a graph of the directivity index as a function of the - 3 dB half angle y_ν.

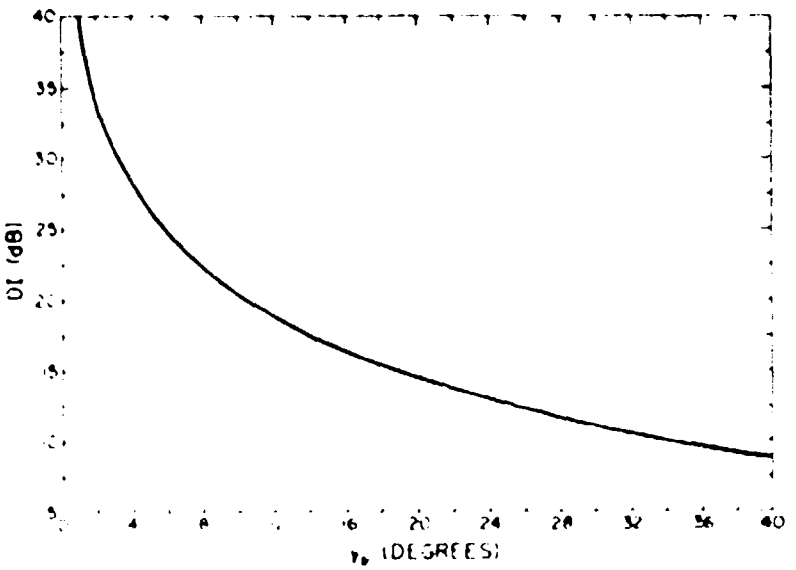

Fig. 9 Directivity index DI in dB as a function of the - 3 dB half angle y_ν in degrees

VOLUME REVERBERATION

Volume reverberation is characterized by an equivalent two-way beam width. The integral expression for this quantity (see e.g., R.J. Urick [6]) is

$$\psi = \int_0^{2\pi} \int_0^{\pi} b(\theta,\phi)\, b'(\theta,\phi) \sin\theta \, d\theta \, d\phi, \tag{12}$$

where $b(\theta,\phi)$ and $b'(\theta,\phi)$ are the beam patterns of the projector and receiver, respectively, and (θ,ϕ) are the standard spherical angles with the z axis being the principle direction of radiation. For the case where $b(\theta,\phi) = b'(\theta,\phi) = P_\nu^2(\cos\theta)$, we have

$$\psi = 2\pi \int_0^{\pi\alpha_\nu/180} P_\nu^4(\cos\theta)\sin\theta d\theta. \tag{13}$$

We rewrite the approximation for $P_\nu(\cos\theta)$ given in Eq. (5) so that θ is in radians and substitute into Eq. (13). Replacing $\sin\theta$ by θ, expanding $J_0(x)$ in the first 3 terms of its power series, multiplying out $J_0^4(x)$, integrating the result term by term, and adding a correction term necessary for low ν, we obtain

$$\psi \simeq 0.000147\alpha_\nu^2(1 + 6.84 \times 10^{-6}\alpha_\nu^2), \tag{14}$$

where α_ν is in degrees. We can also express this in terms of the -3 dB half angle y_ν in degrees:

$$\psi \simeq 0.000670y_\nu^2(1 - 3.65 \times 10^{-5}y_\nu^2), \tag{15}$$

or, expressed in dB,

$$10\log_{10}\psi \simeq 20\log_{10}y_\nu - 31.73 - 1.59 \times 10^{-4}y_\nu^2. \tag{16}$$

This result is nearly identical to that for a circular plane array (circular piston) in an infinite rigid baffle. The inaccuracy in the approximations given in Eqs. (14) and (15) is less than 1%, while that of Eq. (16) is less than 0.1 dB.

SURFACE REVERBERATION

Surface reverberation is characterized by a corresponding two-way beam width Φ given by the integral expression

$$\Phi = \int_0^{2\pi} b(0,\phi)b'(0,\phi)d\phi. \tag{17}$$

For a P_ν CBT projector and receiver:

$$\Phi = 2\int_0^{\pi\alpha_\nu/180} P_\nu^4(\cos\theta)d\theta. \tag{18}$$

Use of the procedure described above in the previous section for obtaining Eq. (14) leads to the following approximation for Φ, accurate to within 1%:

$$\Phi \simeq 0.0123\alpha_\nu(1 + 7.93 \times 10^{-6}\alpha_\nu^2), \tag{19}$$

with α_ν in degrees. We can alternately express Φ in dB accurate to within 0.2 dB in terms of the -3 dB half angle y_ν in degrees:

$$10 \log_{10} \Phi \simeq 10 \log_{10} y_\nu - 15.8 - 9.77 \times 10^{-5} y_\nu^2. \tag{20}$$

This result is about 3 dB lower than the value quoted for the circular plane array by Urick [6] in his Table 8.1. However, a close inspection of the problem reveals that Urick's values for $10 \log_{10} \Phi$ for the circular plane array, the rectangular array, and the horizontal line are all in error by 3 dB. This is probably due to a factor of 2 error in the transcription by Urick of previous results expressed in terms of a surface reverberation index J_s. This surface reverberation index was defined to be $J_s = 10 \log_{10} (\Phi/2\pi)$, as opposed to the volume reverberation index $J_v = 10 \log_{10} (\Psi/4\pi)$.

Evaluation of the surface reverberation for nonzero values of θ is more difficult than for $\theta = 0$. Simple expressions are not likely to exist for this case. Numerical integration appears necessary for each desired value of θ and ν, however, the simplest case of $\nu = 1$ can be solved analytically and yields

$$\Phi(\theta = \theta_0) = \cos^4 \theta_0 \, \Phi(\theta = 0),$$

or

$$\Phi(\theta_0) = P_1^4(\cos \theta_0) \Phi(0), \tag{21}$$

or, in dB,

$$10 \log_{10} \Phi(\theta_0) = 10 \log_{10} \Phi(0) + 40 \log_{10} P_1(\cos \theta_0). \tag{22}$$

Based on this result, we might expect that the more general expression

$$10 \log_{10} \Phi(\theta_0) = 10 \log_{10} \Phi(0) + 40 \log_{10} P_\nu(\cos \theta_0) \tag{23}$$

is a good approximation for small values of θ_0.

IMPLEMENTATION OF THE VELOCITY DISTRIBUTION

As stated earlier, the special radiation properties of the CBT result from the presence of a normal velocity distribution over the outer surface of a spherical cap given by $v(\theta) = P_\nu(\cos \theta)$ for $0 \leq \theta \leq \alpha_\nu$ and $v(\theta) = 0$ for $\theta \geq \alpha_\nu$. The cap half angle must be at least as large as α_ν; to minimize the size and weight of the CBT we choose the cap half angle equal to α_ν. A cross-sectional view of the spherical cap for a P_5 CBT is shown in Fig. 10.

The most obvious choice for the transduction material in the CBT is a piezoelectric ceramic such as lead titanate zirconate. In order to obtain good piezoelectric activity and also to prevent excessive dielectric heating of the ceramic under high power and/or large duty cycle operation, we can use the ceramic composition PZT-4 manufactured by Brush-Clevite, or a similar composition such as Channel 5400 manufactured by Channel Industries,

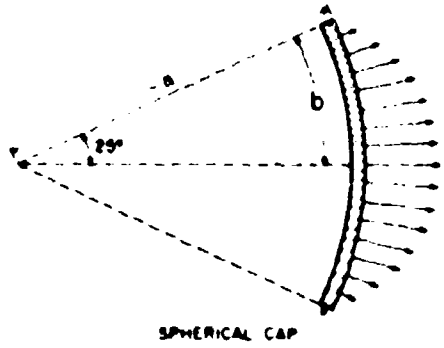

Fig. 10 – Cross-sectional view of the spherical cap for a P_8 CBT. Arrows indicate the relative surface velocity distribution. The cap radius b is measured on the outer spherical surface.

Inc., and TCI-4 manufactured by Marine Resources, Inc. For very high power applications where PZT-4 might overheat, we can substitute a very low-loss composition like PZT-8, although this ceramic is less active than PZT-4.

Experimental results show that it is difficult if not impossible to control the velocity distribution over a spherical cap consisting entirely of a single piece of piezoelectric ceramic. The presence of a variety of mechanical vibration modes in the ceramic cap produces a velocity distribution that is highly frequency dependent. We can avoid this problem by subdividing the ceramic cap into small pieces. We choose the lateral dimensions of each individual ceramic piece small enough so that there are no lateral vibration modes in the frequency band of operation that are sufficiently excited to significantly affect the normal velocity of the piece. We also choose the thickness of the ceramic pieces so that the lowest thickness mechanical resonance occurs well above the maximum operating frequency. The resulting mosaic can be attached to a backing plate that is mechanically rigid enough to maintain the shape of the spherical surface under operating conditions.

It is desirable to mechanically and acoustically isolate the ceramic from the backing plate by a thin layer of decoupling or pressure-release material such as corprene. This prevents the backing plate from vibrating and producing undesired acoustic radiation in the backward ($\theta \approx 180^\circ$) direction. It also prevents the normal velocity distribution from being adversely affected by mechanical resonances that might otherwise be excited in the backing plate. We can also eliminate undesired acoustic radiation from the edges of the piezoceramic pieces by covering them with small strips of corprene.

We believe that corprene can be used as a decoupling material up to a water depth of 300 m without incurring significant changes in performance of the CBT. When the water depth is greater than 300 m, however, the corprene is substantially compressed by the ambient water pressure and becomes too stiff to be effective in decoupling the ceramic from the backing plate. Other decoupling materials suffer from similar limitations. If the required water depth is too great for a pressure-release material to be successful in decoupling the ceramic from the backing plate, the backing plate probably must be made nearly acoustically rigid in order to prevent substantial acoustic radiation in the backward direction. In this case, the backing plate can no longer be lightweight but must be made of material with a large mass density-sound speed product such as steel or tungsten. We assume in this

report that the operating depth requirement does not preclude the use of a decoupling material. The design of a CBT suitable for operating at greater water depths will be deferred for future study.

The inner and outer surfaces of the ceramic pieces are electroded so that a suitable voltage can be applied across them. For maximum electromechanical coupling, each ceramic piece is polarized through its thickness. The resulting normal velocity distribution over the surface of each piece is assumed to be reasonably constant. We can stepwise approximate the continuous velocity distribution $v(\theta) = P_\nu(\cos\theta)$ by driving each ceramic piece with a voltage whose magnitude is proportional to the average value of $P_\nu(\cos\theta)$ over its outer surface. Since the desired CBT velocity distribution is rotationally symmetrical, we first subdivide the spherical cap into N bands, with constant θ boundaries. A natural subdivision scheme to use is one with equal angular-width bands. Numerical calculations show that subdivision into 10 bands of equal angular width results in excellent constant beamwidth behavior over a large frequency range extending from the low cutoff frequency f_c for the continuous velocity distribution to an upper frequency limit f_u that depends on the size of the bands. Alternatively, we can subdivide the cap into N bands of equal area. We determined that eight equal area bands are sufficient to produce constant beamwidth behavior, although the top 2 bands are so much wider than the lower 6 bands that they probably require further subdivision to suppress possible lateral plate modes in the ceramic. Because of the need to suppress lateral plate modes, we recommend that the CBT be subdivided into at least 10 bands whose angular widths are reasonably close to being equal. However, if lateral plate modes are not a problem, any subdivision scheme is acceptable as long as there are at least 8 bands, none of which possesses both an angular width greater than 0.1 α_ν and an area greater than 0.125 times the area of the cap.

The upper frequency limit f_u for a stepped velocity distribution exists because the center of the farfield pattern for the acoustic radiation from a uniformly vibrating band on a sphere exhibits interference maxima and minima as a function of frequency. These extrema occur when the projected height of the band along the axis of the cap, i.e., along the z or polar axis in spherical coordinates, equals an integral number of half wavelengths, $m\lambda/2$. Odd values of m correspond to maxima and even values correspond to minima. A discussion of this effect is given in Ref. 1, although it was erroneously stated there that odd values of m correspond to minima and even values correspond to maxima.

Thus, the central part of the radiation pattern for a CBT consisting of N uniformly shaded bands may differ substantially from the desired constant beamwidth pattern when the frequency is high enough for one or more of the individual bands to exhibit interference extrema. The band with the largest projected height, which is also the band with the largest area, has the lowest extrema frequency. A conservative rule of thumb for the upper frequency limit f_u is 1.5 times the frequency of the first maximum (m=1) for the band of largest area, excluding those bands for which the value of $P_\nu(\cos\theta)$ is less than 0.2. We can express this rule of thumb mathematically by

$$f_u = 0.018\,\alpha_\nu{}^2\, f_c/[(\alpha_\nu + 47.7)(\cos\theta_L - \cos\theta_u)], \tag{24}$$

where f_u and f_c are in the same units, the cap half angle α_ν is expressed in degrees, and θ_L and θ_u are the lower and upper angular limits of the relevant band.

The interference effects described above are predicated on an ideal geometry and a uniform velocity distribution across each band. The extrema might not be very pronounced in the real world of nonideal geometries and nonuniform velocity distributions. In this case, the transducer could possess good constant beamwidth properties well above the frequency f_u. To be on the safe side, however, we recommend subdivision into as many bands as are required to raise f_u, as calculated from Eq. (24), above the highest desired operating frequency. Other factors providing an upper frequency limit for the CBT are discussed in the section called "Bandwidth."

For a closely packed array each band is then driven with a voltage E_i, $i = 1, 2, \ldots N$, proportional to the average of the velocity distribution over the ith band, i.e.,

$$E_i = B \langle P_\nu(\cos\theta) \rangle_i = \frac{2\pi B}{A_i} \int_{\theta_{Li}}^{\theta_{ui}} P_\nu(\cos\theta) \sin\theta d\theta, \tag{25}$$

where θ_{ui} and θ_{Li} are the upper and lower bounds on θ for the ith band, B is the constant of proportionality, and $\langle\rangle_i$ denotes the average over the ith band. The quantity A_i is the solid angle subtended by the ith band and is equal to $2\pi(\cos\theta_{Li} - \cos\theta_{ui})$.

We can evaluate this integral exactly to give

$$E_i = B\left[\frac{P_{\nu+1}(\cos\theta_{Li}) - \cos\theta_{Li} P_\nu(\cos\theta_{Li}) - P_{\nu+1}(\cos\theta_{ui}) + \cos\theta_{ui} P_\nu(\cos\theta_{ui})}{\nu(\cos\theta_{Li} - \cos\theta_{ui})}\right]. \tag{26}$$

Numerical tables of Legendre functions of noninteger order are not readily available, therefore, we express E_i in a trigonometric series by substituting into Eq. (25) the hypergeometric expansion of $P_\nu(\cos\theta)$ in terms of $(1 - \cos\theta)/2$ and integrating term by term. This gives

$$E_i = \frac{B}{\cos\theta_{Li} - \cos\theta_{ui}} \sum_{r=0}^{\infty} \frac{(-1)^r \Gamma(\nu + r + 1)}{r!(r+1)!\Gamma(\nu - r + 1)2^r} \times \left[(1 - \cos\theta_{ui})^{r+1} - (1 - \cos\theta_{Li})^{r+1}\right], \tag{27}$$

where the ratio of gamma functions $\Gamma(\nu + r + 1)/\Gamma(\nu - r + 1)$ equals unity for $r = 0$ and equals the following finite product otherwise.

$$\Gamma(\nu + r + 1)/\Gamma(\nu - r + 1) = (\nu - r + 1)(\nu - r + 2) \ldots (\nu + r), r \neq 0. \tag{28}$$

It is seen from Eq. (28) that the ratio of gamma functions equals zero when ν is an integer and $r > \nu$. In this case the Legendre function $P_\nu(\cos\theta)$ is a polynomial of order ν so that its integral and thus the series of Eq. (27) is a polynomial of order $\nu + 1$. For ν unequal to an integer the series converges rapidly since $\cos\theta_{Li}$ and $\cos\theta_{ui}$ are usually quite close to each other and to unity. Convergence to 4 decimal digits rarely requires more than 6 or

7 terms in the series. There are no approximations involved in Eq. (27); therefore, the error in E_i can be reduced to any desired value by taking enough terms in the series. However, extreme accuracy is unnecessary. Theoretical calculations show that inaccuracies in shading much greater than 1.0% are easily tolerated without significant changes in the radiation properties of a CBT.

We assumed above that the entire outer surface of the cap from $\theta = 0$ to $\theta = \alpha_\nu$ was covered with N distinct bands of ceramic. To suppress possible lateral mechanical modes in the ceramic, we subdivide each band into a number of sufficiently small pieces whose width (extent in the ϕ direction) and height (extent in the θ direction) are comparable. We then connect all the pieces in each band electrically in parallel. This procedure results in each ceramic piece being driven with a voltage proportional to the average value of $P_\nu(\cos\theta)$ over the band in which it is located instead of the average value over the outer surface of the piece itself. We choose to connect the ceramic pieces in parallel in order to optimize the performance of the CBT as a projector. When the CBT is to be used both as a projector and a receiver, or as a receiver alone, it is preferable to use alternative electrical configurations involving both series and parallel connections. We refer the reader to the final paragraphs of the section called "Source Level, Transmitting Voltage and Current Responses, and Receiving Voltage Sensitivity" for a discussion of these alternatives.

If the outer cap surface is not entirely covered with ceramic, then the required voltage shading values E_i' are obtained by dividing the expressions given above in Eqs. (25) to (28) by the packing fractions F_i to obtain $E_i' = E_i/F_i$. The packing fraction F_i is defined to be that fraction of the area of the ith band that is covered by ceramic. If a gap in the ceramic exists between neighboring bands, say between the ith and the $(i+1)$ bands, then both the lower bound $\theta_{L,i+1}$ on the upper band and the upper bound θ_{ui} on the lower band should be assumed to lie exactly in the middle of the gap. If it is necessary to leave significant gaps between ceramic pieces, the gaps should be filled with a nearly mechanically rigid material such as tungsten. Of course, the edges of the ceramic pieces should still be covered with small strips of coprene to eliminate edge radiation. We strongly encourage the designer of a CBT to use a close-packed ceramic mosaic. This avoids the need for filler material and provides the maximum probability of success.

The required voltage values E_i can be obtained experimentally by several methods. One method is to use individual phase-locked amplifiers, one for each band. An easier method is to connect a shading capacitor suitable for power applications in series with each of the bands except the first or topmost band, and then to connect all of the band-capacitor combinations in parallel with the first band. A single power amplifier is then sufficient to drive the entire CBT mosaic. The capacitors act as voltage dividers to provide the desired voltage values. It is convenient to normalize the set of values E_i', $i = 1,2,\ldots N$, by E_1' and call the resulting numbers $w_i = E_i'/E_1' = F_1E_i/(F_iE_1)$, $i = 1,2,\ldots N$, the CBT shading coefficients. The required shading capacitance values C_i for bands 2, 3,..., N are given in terms of w_i by

$$C_i = C_1^E w_i/(1 - w_i), \tag{29}$$

where C_i^F is the stress-free ceramic capacitance of the ith band. For the usual case where all the ceramic pieces in the ith band are of uniform thickness l_i and cover a combined area on the spherical cap equal to $F_i A_i a^2 = F_i A_i b^2 / [\pi^2 \alpha_\nu^2 / (180)^2]$, with $A_i = 2\pi (\cos \theta_{Li} - \cos \theta_{ui})$, we have (neglecting fringing fields)

$$C_i^F = \frac{K_{33}^T \epsilon_0 F_i A_i b^2}{l_i [\pi^2 \alpha_\nu^2 / (180)^2]}. \tag{30}$$

Here, α_ν is in degrees, K_{33}^T is in the stress-free relative dielectric constant, and $\epsilon_0 = 8.85 \times 10^{-12}$ F/m is the dielectric constant of free space. For PZT-4, K_{33}^T is approximately equal to 1300.

SIZE AND MASS

In order to determine the radius b of the spherical cap (i.e., the half arclength, not to be confused with the radius of curvature a of the cap) required for a CBT, we need first to specify the desired beam pattern. Typical choices for specifying the beam pattern are the -3 dB half angle y_ν or the total beam half angle α_ν. The order ν of the Legendre function shading corresponding to y_ν or α_ν can be calculated using the following approximations (accurate to within 0.1% for $\alpha_\nu \lesssim 90°$ and $y_\nu \lesssim 45°$):

$$\nu \simeq \left(\frac{64.540}{y_\nu}\right)\left(1 + 2.26 \times 10^{-5} y_\nu^2\right) - 0.5 \tag{31a}$$

and

$$\nu \simeq \left(\frac{137.796}{\alpha_\nu}\right)\left(1 - 2.43 \times 10^{-6} \alpha_\nu^2\right) - 0.5. \tag{31b}$$

We must next specify the lowest desired operating frequency f_c of the CBT. We can now calculate the required cap radius in meters by use of

$$b = c\left(1.10 + \frac{24.6}{y_\nu}\right)/(1500 f_c) \tag{32a}$$

or

$$b \simeq c[1.10 + (52.5/\alpha_\nu)(1 - 7.79 \times 10^{-6} \alpha_\nu^2)]/(1500 f_c), \tag{32b}$$

where the sound speed c of the surrounding fluid is in m/s, f_c is in kHz, and y_ν and α_ν are in degrees.

The required thickness of the ceramic does not depend on f_c, and consequently not on the cap radius b. Thus, the total mass of ceramic increases linearly with area. We assume in this section that the entire spherical cap $0 \le \theta \le \alpha_\nu$ is covered with ceramic. The area of a spherical cap of half angle α_ν is given by $\mathcal{A} = 2\pi a^2 (1 - \cos \alpha_\nu)$, where a is the radius

of curvature of the cap. We can approximate the cap area by its upper bound πb^2 obtained by expanding $\cos \alpha_\nu$ in a power series in α_ν and retaining only the first two terms. The error in this approximation decreases as α_ν decreases; it is nearly 23.4% for $\alpha_1 = 90°$ but decreases to less than 8% for $\alpha_2 = 54.74°$. Thus, for $\nu \geq 2$ the ceramic mass varies nearly quadratically with the cap radius.

We assume that the ceramic is of uniform thickness over the entire cap and obtain for its mass M_c in kg:

$$\begin{aligned} M_c &= \rho_c \ell \mathcal{A} \\ &= 2\pi\rho_c \ell b^2 (1 - \cos \alpha_\nu)/[\pi\alpha_\nu/180]^2, \end{aligned} \tag{33}$$

or, in terms of the lower cutoff frequency f_c by use of Eq. (32b),

$$M_c \simeq 2\pi\rho_c \ell c^2 [1.10 + (52.5/\alpha_\nu)(1 - 7.79 \times 10^{-6}\alpha_\nu^2)]^2 (1 - \cos \alpha_\nu)/[25\pi f_c \alpha_\nu/3]^2, \tag{34}$$

where ρ_c is the mass density of the ceramic in kg/m^3, c is the sound speed of the surrounding fluid in m/s, ℓ is the ceramic thickness in meters, α_ν is in degrees, and f_c is in kHz. We can also express the mass in terms of the - 3 dB half angle y_ν in degrees as

$$M_c \simeq \pi\rho_c \ell c^2 [1.10 + (24.6/y_\nu)]^2 (1 - 1.16 \times 10^{-4} y_\nu^2)/(1500/f_c)^2. \tag{35}$$

In Fig. 11 we present a graph of M_c as a function of y_ν for the case where the surrounding fluid is water, the ceramic is PZT-4 ($\rho_c \sim 7500$ kg/m^3), $\ell = 0.001$ m, and $f_c = 10$ kHz. The ceramic mass M_c for other choices of ℓ in m and f_c in kHz can be obtained from this graph by multiplying the plotted values by $10^5(\ell/f_c^2)$.

The section after next will show that the transmitting voltage response of a CBT does not depend on the thickness of the ceramic. However, the thickness does determine the maximum achievable source level since it limits the maximum voltage that can be applied to the CBT. When series shading capacitors (see the section, "Implementation of the Velocity Distribution") are used as voltage dividers to reduce the voltage across all but the topmost ceramic band, the thickness of the ceramic in these bands can be reduced in proportion to the voltage reduction without reducing the maximum achievable source level. We then have $\ell_i = E_i \ell_1 / E_1$, and the ceramic mass becomes

$$M_c' = (E_T/E_1) M_c, \tag{36}$$

where M_c is given by Eqs. (33) to (35), E_1 is given by Eqs. (25) to (28) with $i = 1$, and E_T is proportional to the average of $P_\nu(\cos \theta)$ over the entire cap, and is given by Eqs. (25) to (28), with $\theta_{Li} = 0$ and $\theta_{ui} = \alpha_\nu$. It can be shown that E_T is well approximated by $0.432B[1 + 0.356/(\nu + 0.5)^2]$, and that for the case of eight or more bands, $B > E_1 > 0.91B$. Thus, we have

$$M_c' < 0.48[1 + 0.356/(\nu + 0.5)^2] M_c, \tag{37}$$

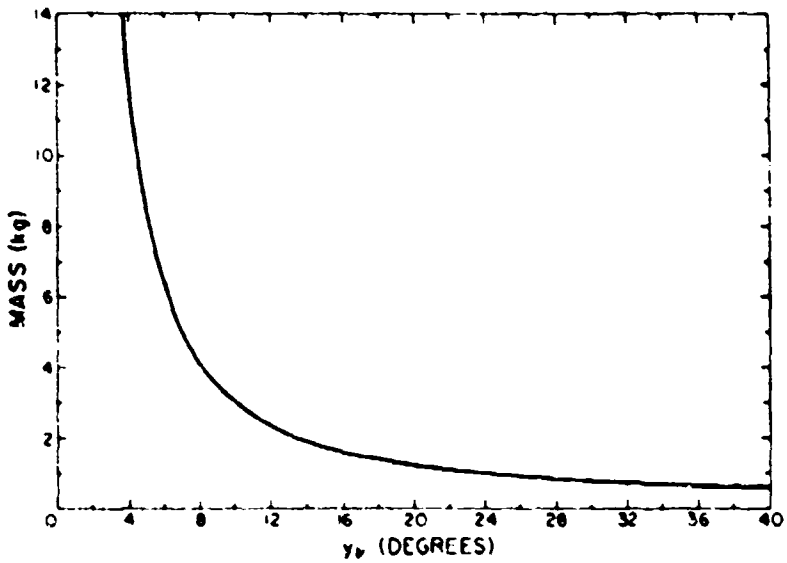

Fig. 11 — Mass of the ceramic required in a CBT in kg as a function of the -3 dB half angle γ_b in degrees for a lower cutoff frequency of 10 kHz and for a ceramic thickness of 0.001 m

so that the reduction in mass of the ceramic is approximately 50%, however, the input electrical impedance of the CBT and, consequently, both the transmitting current response and the receiving voltage sensitivity are also reduced by the same factor.

If the CBT will not be used at water depths greater than about 300 m the backing plate can be made reasonably light weight and will not add substantially to the weight of the CBT in water. In this case, the only design requirement for the backing plate is to maintain the shape of the spherical cap. We estimate that the entire mass of the CBT with a light weight backing plate will be less than twice that of the ceramic alone. In addition, the use of low-mass-density materials such as plastics in the backing plate should result in a CBT weight in water that is barely larger than that of the ceramic.

If the CBT must be used at great depths so that corprene or another good pressure-release material cannot be used to decouple the ceramic from the backing plate, the backing plate must be made of a material such as steel or tungsten and will greatly increase the mass and weight of the CBT.

BANDWIDTH

The bandwidth of a CBT is determined by several factors. The lower frequency limit f_c (in kHz) depends on the cap radius b (in meters), the sound speed c of the surrounding

fluid (in m/s), and the - 3 dB half angle y_v or, alternatively, the cap half angle α_v (in degrees) according to the following two formulas (given earlier):

$$f_c = c\left(1.10 + \frac{24.6}{y_v}\right)/(1500b), \tag{9a}$$

$$f_c \simeq c[1.10 + (52.5/\alpha_v)(1 - 7.79 \times 10^{-6}\alpha_v^2)]/(1500b). \tag{9b}$$

A reduction in f_c for the same desired beam pattern (α_v = constant or y_v = constant) requires a corresponding increase in b and a resulting increase in the mass and weight of the CBT (see section called "Size and Mass").

There are two primary factors that determine the upper frequency limit. The first factor is the size of the constant-velocity bands used in stepwise implementing the velocity distribution. If one or more of the bands is too large for the desired high frequency limit, interference extrema can significantly degrade the center of the farfield radiation pattern at frequencies within the operating band. We discuss this effect in detail in the "Implementation of the Velocity Distribution" section. An estimate of the upper frequency limit for a given velocity band subdivision scheme is given by Eq. (24).

The second factor that determines the frequency limit is the shape and size of the ceramic pieces used in the mosaic. If the pieces are not identical in shape and size, the upper frequency limit for constancy of both the beam pattern and the transmitting current response is somewhat less than the fundamental thickness resonance of the thickest piece. On the other hand, if the pieces are identical they will respond identically with frequency since the acoustic loading is uniform over the entire spherical cap. In this case, the occurrence of a resonance will affect the surface normal velocity magnitude but not its distribution, and, thus, the beam pattern will remain constant. Of course, the transmitting current response will follow the frequency dependence of the velocity magnitude, increasing somewhat as the fundamental thickness resonance is approached, and decreasing rapidly above resonance. This rapid decrease in response above resonance places a practical limit on the upper frequency limit of the CBT.

SOURCE LEVEL, TRANSMITTING VOLTAGE AND CURRENT RESPONSES, AND RECEIVING VOLTAGE SENSITIVITY

The on axis ($\theta = 0°$) farfield acoustic pressure produced by the CBT at a distance R at a frequency well above its cutoff frequency is shown in [1] to be

$$P_{FF} = (\rho c U_0 a/R)e^{jk(R-a)}e^{-j\omega t}, \tag{38}$$

where ρ and c are the density and sound speed of water or whatever fluid the CBT is radiating into, a is the radius of curvature of the spherical cap, $\omega = 2\pi f$ is the angular frequency, and U_0 is the normal velocity of the transducer surface at $\theta = 0°$, i.e., in the center of the cap. We assume in the following discussion that the transducer consists of a close-packed mosaic of small ceramic elements that are decoupled from a backing plate by

pressure release material. We also assume that the frequency is well below the fundamental or lowest thickness resonance of the ceramic.

If the individual ceramic pieces have lateral dimensions that are small relative to the wavelength of sound in the ceramic, then the velocity U_0 is given by

$$U_0 = -i\omega d_{33} E_0/2. \tag{39}$$

Here, d_{33} is a piezoelectric constant of the ceramic and E_0 is the input voltage to the CBT. On the other hand, if the lateral dimensions are large compared to a wavelength, the factor d_{33} in Eq. (39) must be replaced by $K_{33}^T \epsilon_0 h_{33}/c_{33}^D$, where K_{33}^T, h_{33}, and c_{33}^D are dielectric, piezoelectric, and elastic constants, respectively, of the ceramic. For a description of these constants together with numerical values representative of selected ceramic compositions, we refer the reader to Ref. 7. In general, $d_{33} > K_{33}^T \epsilon_0 h_{33}/c_{33}^D$, so the normal velocity obtained with a given input voltage is greater when d_{33} is appropriate. For example, using the following typical values for PZT-4 given in Ref. 7: $K_{33}^T = 1300$, $d_{33} = 2.89\times10^{-10}$ m/V, $h_{33} = 2.68\times10^{9}$ V/m, and $c_{33}^D = 1.59\times10^{11}$ N/m^2, we find that $K_{33}^T \epsilon_0 h_{33}/c_{33}^D = 1.94\times10^{-10}$ m/V, which is 33% less than d_{33}. We assume in the following discussion that d_{33} is the appropriate factor for the CBT for all but possibly the upper end of the operating frequency range.

Substituting for U_0 from Eq. (39) into Eq. (38), replacing a by $b/(\pi\alpha_\nu/180)$, setting R equal to 1 m, and ignoring the phase terms, we obtain the following equation for the farfield pressure magnitude referenced to 1 m:

$$|P_{FF}(R = 1\text{ m})| = \rho c b \omega d_{33} E_0/(2\pi\alpha_\nu/180). \tag{40}$$

Thus, the source level of the CBT in dB ref. 1μPa at 1 m is given by

$$SL = 20\log_{10}[\rho c b \omega d_{33} E_0/(2\pi\alpha_\nu p_0/180)], \tag{41}$$

where p_0 is the reference pressure equal to 1μPa at 1 m.

The maximum achievable source level is limited by the maximum electric field that can be applied to the ceramic before dielectric failure or depolarization occurs. This depends on the duty cycle used and can be larger than 10^5 volts per centimeter of ceramic thickness for very low duty cycles. However, for most sonar applications it is desired that the pressure waveform produced in the water be linearly related to the applied voltage waveform. In this case, the applied electric fields must be less than about 2000 V/cm in order to be small compared to the DC electric fields used to polarize the ceramic during its initial preparation. This results in a somewhat lower usable source level. We can alternately express the source level in terms of the dimensionless frequency ratio f/f_c and the -3 dB half angle y_ν by use of Eqs. (2), (3) and (32a):

$$SL \simeq 20\log_{10}\left[10^6 \rho c^2 d_{33} E_0 \left(0.618 + \frac{13.8}{y_\nu}\right)\left(1 + 3.55\times10^{-5} y_\nu^2\right)\left(f/f_c\right)/y_\nu\right]. \tag{42}$$

This expression is evaluated using MKS values for ρ, c, and d_{33}, and expressing y_v in degrees. We note that the source level of the CBT increases linearly with frequency over its operating band, the minimum value occurring at the lower cutoff frequency.

The transmitting voltage response S_V in $\mu Pa/V$ is found from Eq. (42) to be

$$S_V \simeq 10^8 \rho c^2 d_{33} \left(0.618 + \frac{13.8}{y_v}\right)\left(1 + 3.55 \times 10^{-5} y_v^2\right)\left(f/f_c\right)/y_v. \tag{43}$$

For the case of water and PZT-4, with $\rho = 1000$ kg/m^3, $c = 1500$ m/s, and $d_{33} = 2.89\times10^{-10}$ m/V, we have

$$S_V \simeq 3.65 \times 10^7 \left(1.10 + \frac{24.6}{y_v}\right)\left(1 + 3.55 \times 10^{-5} y_v^2\right)\left(f/f_c\right)/y_v. \tag{44}$$

The minimum transmitting voltage response over the operating band $S_{V,MIN}$ is given for this case in dB ref 1 $\mu Pa/V$ by the approximation

$$S_{V,MIN} \simeq 151.2 + 20 \log_{10}\left[\left(1.10 + \frac{24.6}{y_1}\right)\left(1 + 3.55 \times 10^{-5} y_1^2\right)/y_v\right]. \tag{45}$$

We present in Fig. 12 a graph of $S_{V,MIN}$ as a function of the - 3 dB half angle y_1.

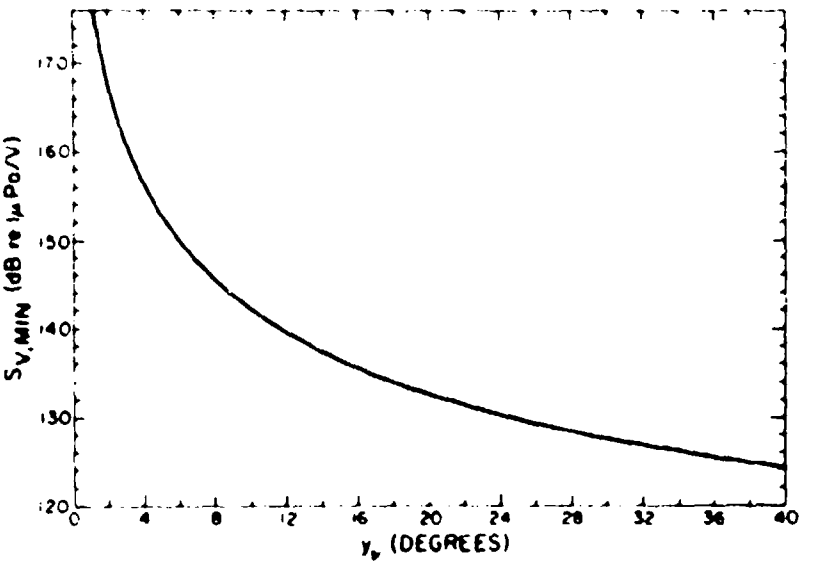

Fig. 12 — Minimum transmitting voltage response $S_{V,MIN}$ in dB ref 1 $\mu Pa/V$ as a function of the - 3 dB half angle y_v in degrees

The transmitting current response S is obtained from S_V by use of

$$S = |Z| S_V \tag{46}$$

where Z is the input electrical impedance to the CBT. For frequencies well below mechanical resonance, $Z \simeq 1/i\omega C_T$, where C_T is the total electrical capacitance of the CBT under stress-free boundary conditions. When the velocity shading is achieved by the use of shading capacitors as described in the section on "Implementation of the Velocity Distribution," the total capacitance can be obtained using Eqs. (25), (29), and (30), and is given by

$$C_T = \frac{2\pi K_{33}^T \epsilon_0 F_1 b^2}{|\pi\alpha_\nu/180|^2 \langle P_\nu(\cos\theta)\rangle_1} \sum_{i=1}^{N} \frac{1}{l_i} \int_{\theta_{Li}}^{\theta_{ui}} P_\nu(\cos\theta)\sin\theta d\theta, \tag{47}$$

where l_i is the ceramic thickness of the ith band (assumed to be uniform over the band). The appearance in the denominator of the average of $P_\nu(\cos\theta)$ over the first band is due to the normalization of the shading coefficients w_i so that $w_1 = 1.0$.

For the case that $l_1 = l_2 = \cdots = l_N = l$, we can remove l_i from the sum and combine the individual band integrals into a single integral I over the entire spherical cap from $\theta = 0$ to $\theta = \alpha_\nu$. This integral can be evaluated by using Eqs. (27) and (28) to calculate E_i for $\theta_{Li} = 0$ and $\theta_{ui} = \alpha_\nu$, and then using the relationship $I = (1 - \cos\alpha_\nu) BE_i$ obtained from Eq. (25). The quantity $\langle P_\nu(\cos\theta)\rangle_1 = E_1/B$ can also be evaluated using Eqs. (27) and (28). However, simpler expressions can be obtained for I and $\langle P_i(\cos\theta)\rangle_1$ by using the approximation for $P_\nu(\cos\theta)$ given in Eq. (5), replacing $\sin\theta$ by θ, and integrating the resulting expressions exactly. After some further algebra plus the addition of an empirically determined correction factor, we obtain the approximation:

$$C_T \simeq \frac{1.36\, K_{33}^T \epsilon_0 F_1 b^2}{l} (1 - 3.24\times10^{-5} y_\nu^2)\left[1 + 0.72\left(\frac{\theta_{u1}}{\alpha_\nu}\right)^2\right], \tag{48}$$

where all angles are in degrees. This approximation is believed to be accurate to within 1% for $\nu \geq 1$. The bracketed factor in Eq. (48) can be approximated by $1 + (0.72 A_1/A)$, where $A_1/A = (1-\cos\theta_{u1})/(1-\cos\alpha_\nu)$ is the fraction of the total cap area covered by the first or topmost band. The inaccuracy in this approximation is less than about 1% for $\pi\alpha_\nu/180 \leq 1$, i.e., for $\nu \geq 2$. If there are N bands of equal area, $A_1/A = 1/N$.

An excellent approximation for the transmitting current response S in units of $\mu Pa/A$ and in terms of y_ν and f_c is obtained by combining Eqs. (32a), (43), (46), and (48):

$$S \simeq \frac{1.48\times10^{10}\rho\, l d_{33} f_c (1 + 6.79\times10^{-5} y_\nu^2)}{K_{33}^T \epsilon_0 F_1 (1.10 y_\nu + 24.6)}\left[1 - 0.72\left(\frac{\theta_{u1}}{\alpha_\nu}\right)^2\right], \tag{49}$$

where f_c is in kHz. We note that S is independent of the operating frequency. For the case of water as the surrounding fluid, PZT-4 as the ceramic, a packing fraction of unity for the

first band ($F_1 = 1.0$), and the ratio $(\theta_{a1}/\alpha_\nu)^2$ equal to 0.125, such as would be obtained approximately with 8 equal area bands, we have:

$$S \simeq 3.38 \times 10^{11} \frac{\ell f_c (1 + 6.79 \times 10^{-5} y_\nu^2)}{(1.10 y_\nu + 24.6)} . \tag{50}$$

Figure 13 shows the behavior of S in dB ref. 1 $\mu Pa/A$ as a function of the -3 dB half angle y_ν for $\ell = 0.001$ m and $f_c = 10$ kHz. Values of S for other choices of ℓ and f_c can be obtained from Fig. 13 by adding the factor $20 \log_{10}(\ell f_c/0.01$ kHz·m) to the plotted values.

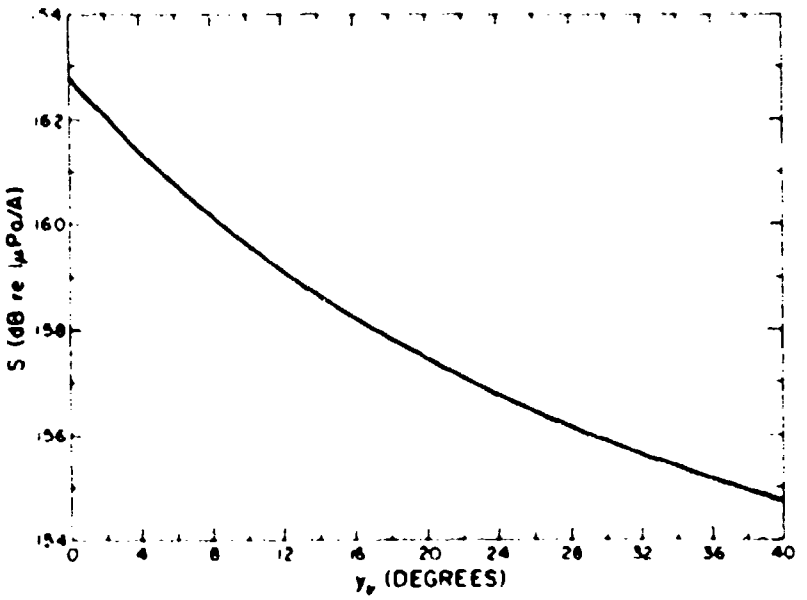

Fig 13 – Transmitting current response S in dB ref 1 $\mu Pa/A$ as a function of the -3 dB half angle y_ν in degrees for $\ell = 0.001$ m and $f_c = 10$ kHz

The receiving voltage sensitivity M in $V/\mu Pa$ is found from S in $\mu Pa/A$ by using the relation $M = 10^{-12} JS$, where $J = 0.002/\rho f$ is the spherical reciprocity factor when f is in kHz:

$$M = \frac{2.96 \times 10^{-5} \ell d_{33} (f_c/f)(1 + 6.79 \times 10^{-5} y_\nu^2)}{K_{33}^T \epsilon_0 F_1 (1.10 y_\nu + 24.6)} \left[1 - 0.72 \left(\frac{\theta_{a1}}{\alpha_\nu}\right)^2\right] . \tag{51}$$

Thus, for frequencies well below resonance, the receiving voltage sensitivity of the CBT is a maximum at the cutoff frequency and decreases linearly with increasing frequency above that point. We obtain, for the case of water, PZT-4, $F_1 = 1.0$, and $(\theta_{a1}/\alpha_y)^2 = 0.125$,

$$M = 6.75 \times 10^{-7} \frac{\ell(f_c/f)(1 + 6.79 \times 10^{-5} y_y^2)}{(1.10 y_y + 24.6)} . \tag{52}$$

In Fig. 14, we plot the behavior of the maximum receiving voltage sensitivity M_{MAX}, i.e., M at $f = f_c$, as a function of the - 3 dB half angle y_y for this case with $\ell = 0.001$ m. Values of M_{MAX} for other choices of ℓ can be obtained from Fig. 14 by adding $20 \log_{10}(\ell/0.001\ \text{m})$ to the plotted values.

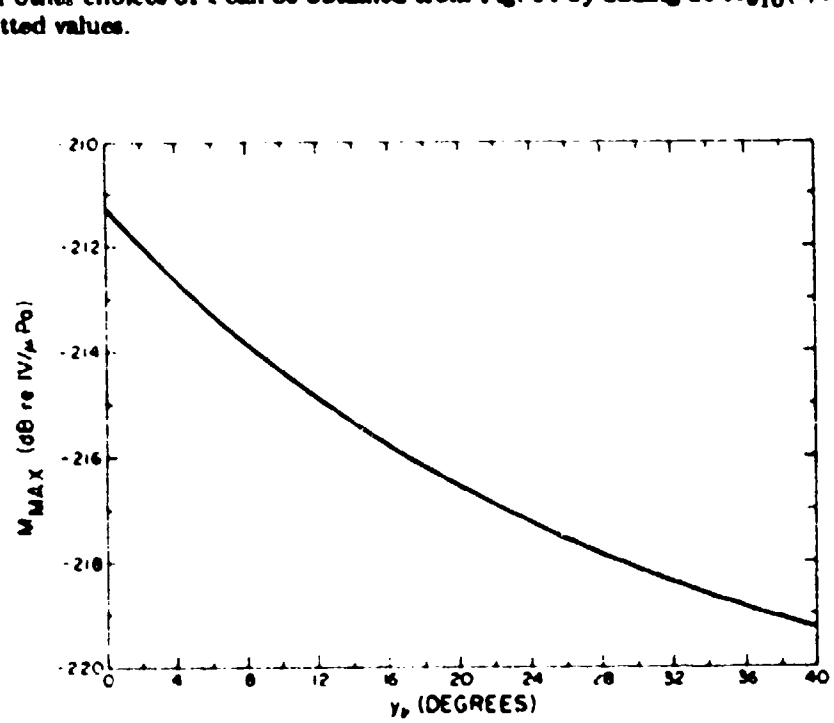

Fig. 14 - Maximum receiving voltage sensitivity M_{MAX} in dB ref 1 V/μPa as a function of the - 3 dB half angle y_y in degrees for $\ell = 0.001$ m

We note that the receiving voltage sensitivity depends weakly on (θ_{a1}/α_y) through the bracketed factor in Eq. (51). Since the CBT mosaic should never be subdivided so that the area of the first band exceeds 1/8 the area of the entire cap, the factor $(\theta_{a1}/\alpha_y)^2$ is never greater than 0.125 and, thus, the bracketed factor has a minimum value of 0.91. Both the expression for M given in Eq. (52) and the values for M_{MAX} plotted in Fig. 14 represent this minimum.

The somewhat low receiving voltage sensitivity values shown in Fig. 14 are due primarily to the relatively low input electrical impedance of the CBT which results from

connecting the individual pieces of ceramic in the mosaic in parallel. The use of parallel connections maximizes the transmitting voltage response; however, it simultaneously minimizes the input electrical impedance, the transmitting current response, and the receiving voltage sensitivity.

If the CBT is to be used as a receiver, we can increase the receiving voltage sensitivity by the use of series electrical connections. The easiest procedure to gain receiving voltage sensitivity involves changing the electrical connections between the N bands from parallel to series while retaining the parallel connections between all the pieces of ceramic in each band. In this case we obtain the CBT amplitude shading, $w_i = F_1 E_i / F_i E_1$, $i = 1,2,\ldots N$, by connecting a shading capacitor in parallel with each band except the first. The required shading capacitance values C_i', $i = 2,3,\ldots N$, are given by

$$C_i' = (C_1^F - w_i C_i^F)/w_i, \tag{53}$$

where C_i^F is the stress-free ceramic capacitance of the ith band. We note that C_i' will be nonnegative and, hence, physically realizable only if $C_1^F \geq w_i C_i^F$. This condition is obviously satisfied by a close packed mosaic of uniform thickness ceramic and equal area bands where $C_i^F = C_1^F$ and $w_i \leq 1$ for all i. If the condition is not satisfied, a shading capacitor C_1' chosen so that $C_1^F + C_1' \geq w_i C_i^F$ for all $i \neq 1$ must be added in parallel with the first band.

The series-parallel arrangement described above results in an increase in the receiving voltage sensitivity over that of the original parallel arrangement by the factor $\sum_{i=1}^{N} w_i C_i^F / (C_1^F + C_1')$. This increase is accompanied by a corresponding decrease in the transmitting voltage response by the factor $1/\sum_{i=1}^{N} w_i$ and an increase in the electrical impedance (at frequencies well below resonance) by the factor $[\sum_{i=1}^{N} w_i C_i^F/(C_1^F + C_1')] \sum_{j=1}^{N} w_j$.

When all the ceramic has the same thickness and when $C_1' = 0$, we have

$$\sum_{i=1}^{N} w_i C_i^F / C_1^F = \frac{\sum_{i=1}^{N} E_i A_i}{E_1 A_1} = \frac{\int_0^{\alpha_v} P_\nu(\cos\theta)\sin\theta\, d\theta}{\int_0^{\theta_{w1}} P_\nu(\cos\theta)\sin\theta\, d\theta}. \tag{54}$$

An excellent approximation for this factor is given by

$$\sum_{i=1}^{N} w_i C_i^F / C_1^F \simeq \frac{0.432(1 - \cos\alpha_v)[1 + 0.356/(\nu + 0.5)^2]}{(1 - \cos\theta_{w1})[1 - 0.72(\theta_{w1}^2/\alpha_v^2)]}. \tag{55}$$

Neglecting the bracketed quantity in the numerator of Eq. (55), which becomes insignificant at large ν or small α_ν, we obtain, for the case of N equal area bands:

$$\sum_{i=1}^{N} w_i C_i^F / C_1^F = \sum_{i=1}^{N} w_i \simeq 0.432\, N[1 + (0.72/N)]. \tag{56}$$

In this case, the gain in the receiving voltage sensitivity varies nearly linearly with the number of bands. For the minimum eight equal area bands, the receiving voltage sensitivity increases 11.5 dB. At the same time, the transmitting voltage response decreases 11.5 dB, and the input electrical impedance increases 23.0 dB.

We can also increase the receiving voltage sensitivity of the CBT by connecting the pieces of ceramic in each band in series instead of in parallel. However, care must be taken to insure the required CBT amplitude shading. The most straightforward procedure is to subdivide each band in the ϕ dimension into L identical pieces. The L pieces in each band are then connected in series electrically. With this method, we simultaneously increase the receiving voltage sensitivity and decrease the transmitting voltage response in dB by $20 \log_{10} L$.

A decrease in the transmitting voltage response due to series connections will not decrease the maximum achievable source level if the CBT can handle the larger input voltages that are required. The resulting voltage across each ceramic piece remains unchanged for a given source level.

EXAMPLE

As an example, we consider the design of a CBT which is to be used both as a projector and a receiver and which meets the following requirements:

1. -3 dB half angle: $y_{\frac{1}{2}} = 7°$
2. Frequency range: 15-100 kHz
3. Source level: SL $\geq$ 200 dB re 1 μPa at 1 m
4. Receiving voltage sensitivity at 15 kHz: $M_{MAX} \geq$ - 200 dB re 1 V/μPa
5. Water depth capability: 300 m

We calculate the required CBT design parameters as follows:

1. The Legendre function order, from Eq. (31a): $\nu = 8.73$.
2. The cap half angle, from Eq. (2): $\alpha_{8.73} = 14.92°$.
3. The cap radius, from Eq. (32) with $f_c = 15$ kHz: $b = 0.308$ m.

4. The minimum transmitting voltage response, from Eq. (45); $S_{V,MIN}$ = 147.6 dB re 1 $\mu Pa/V$.

5. The maximum input voltage required to obtain a source level of 200 dB re 1 μPa at 1 m is given by V_{MAX} = (200-147.6) dB re 1 V or V_{MAX} = 417V. This is the voltage required at 15 kHz. The voltage required for a source level of 200 dB re 1 μPa at 1 m decreases linearly with frequency, falling to 62.6 V at 100 kHz.

6. We choose PZT-4 or equivalent as the ceramic composition and assume a close-packed mosaic. For 8 equal area shading bands, uniform ceramic thickness, and all parallel electrical connections, the receiving voltage sensitivity at the cutoff frequency for 1 mm of ceramic thickness is found from Eq. (52) to be - 213.6 dB re 1 $V/\mu Pa$. Thus - 200 dB requires a ceramic thickness ℓ = 4.79 mm. This thickness is sufficiently large to prevent overheating or nonlinearity in the ceramic even when the maximum required driving voltage of 417 V is applied continuously. The receiving voltage sensitivity will decrease linearly with frequency, being equal to - 216.5 dB re 1$V/\mu Pa$ at 100 kHz. If desired, a differentiating circuit can be used in the receiving electronics to remove this frequency dependence.

7. The input electrical impedance at the cutoff frequency, $Z_{f_c} = 1/(2\pi f_c C_T)$, from Eq. (48), with $(\theta_{a1}{}^2/\alpha_v{}^2) = 0.125$; Z_{f_c} = 31.5 Ω. The impedance will decrease linearly with frequency, being equal to 4.7 Ω at 100 kHz.

8. The required input current for a source level of 200 dB re 1 μPa at 1 m is given by $I = V_{MAX}/Z_{f_c}$ = 13.2 A. Since the transmitting current response is nearly flat with frequency, a nearly constant source level of 200 dB re 1 μPa at 1 m is obtained over the entire frequency band by use of a constant current drive of 13.2 A.

9. The upper frequency limit of 100 kHz is well below the lowest thickness resonance of the ceramic which is approximately equal to 460 kHz.

10. The mass of the ceramic, from Eq. (35) with ρ_c = 7500 kg/m^3; $M_c \simeq$ 10.7 kg. Thus, the entire CBT should weigh less than 22.7 kg (50 lb) in air. Its weight in water can be substantially less than this since a low-mass-density backing plate can be used in its construction.

11. For 8 equal area bands, the angular limits are given by $\theta_{ui} = \theta_{L,i+1} = \cos^{-1}\{1 - (i/8)(1 - \cos\alpha_{8,73})\}$. We obtain θ_{ui}, i = 1, 2, ..., 8, = 5.26°, 7.44°, 9.12°, 10.54°, 11.78°, 12.91°, 13.95°, and 14.92°. The CBT need not be constructed with precisely these angular limits. If 8 bands are used, the actual angular limits can differ slightly from these values as long as the individual band areas do not differ more than about 5%. On the other hand, if more than 8 bands are used, the only restriction is that no band be larger in area than 1/8 the area of the cap.

12. For 8 equal area bands, the CBT shading coefficients are obtained using Eqs. (27) and (28) together with the definition $w_i = E_i/E_1$. The result: w_i, i = 1, 2, ..., 8, = 1.000, 0.821, 0.657, 0.508, 0.373, 0.252, 0.148, and 0.0451.

13. The required shading capacitors C_i should be determined from Eq. (29) using experimental values for the stress-free capacitance of each band C_i^F measured after the CBT mosaic has been constructed. We can obtain approximate values for C_i in the case of 8 equal area bands by using $C_i^F = C_T/8$ with C_T given by Eq. (48). The result is: C_i, $i = 2, 3, \ldots, 8 = 0.197\ \mu F$, $0.0829\ \mu F$, $0.0444\ \mu F$, $0.0257\ \mu F$, $0.0145\ \mu F$, $7150\ \mu\mu F$, and $1990\ \mu\mu F$. Inaccuracies of at least 1% in the shading capacitances can be tolerated without degrading the performance of the CBT.

SUMMARY

We have presented design formulas for a constant beamwidth transducer based on Legendre function amplitude shading of a spherical cap. Included are simple algebraic and trigonometric expressions for the required velocity distribution, limiting beam pattern, directivity index, equivalent two-way beamwidths for volume and surface reverberation, shading coefficients for a stepwise implementation of the velocity distribution, spherical cap size, ceramic mass, bandwidth, source level, transmitting voltage and current responses, and receiving voltage sensitivity. Most of the expressions are approximations for difficult-to-evaluate expressions in terms of Legendre function of fractional order. The approximations are extremely accurate, involving substantially less inaccuracy than is normally encountered in transducer construction.

The formulas are restricted to constant beamwidths whose - 3 dB half angle is no greater than 45°. This corresponds to restricting the order of the Legendre function to be unity or greater. The restriction is somewhat arbitrary; it was made in order to simplify the approximations. If a need arises for a CBT with a - 3 dB half angle greater than 45°, then expressions corresponding to but more complicated than those given in this report can be obtained for a Legendre function order less than unity.

ACKNOWLEDGMENT

We gratefully acknowledge valuable discussions with Mr. T. A. Henriquez during the preparation of this manual.

REFERENCES

1. P.H. Rogers and A.L. Van Buren, "New Approach to a Constant Beamwdith Transducer," *J. Acoust. Soc. Am.* 64:38-43 (1978)

2. W.J. Trott, "Design Theory for a Constant-Beamwidth Transducer," NRL Report 7933 (1975)

3. M. Abramowitz and I.A. Stegun, *Handbook of Mathematical Functions*, NBS Applied Mathematics Series No. 55, Wash., D.C. (1965) p. 369

4. E. Jahnke and F. Emde, *Tables of Functions with Formulae and Curves*, 4th ed., Dover Publications, New York (1945) p. 156

5. Harvard Computation Laboratory, *Tables of the Bessel Functions of the First Kind of Orders Zero and One*, Vol. 3, Harvard University Press, Cambridge, Mass., (1947)

6. R.J. Urick, *Principles of Underwater Sound*, 2nd ed., McGraw-Hill, New York (1975) p. 217

7. D.A. Berlincourt, D.R. Curran, and H. Jaffe, "Piezoelectric and Piezomagnetic Materials and Their Function in Transducers," Chapt. 3 in *Physical Acoustics, Principles and Methods*, Vol. I – Part A (ed. by W.P. Mason), Academic Press, New York (1964)